Available online at www.sciencedirect.com

ScienceDirect

Developmental Biology 296 (2006) 499–513

DEVELOPMENTAL BIOLOGY

www.elsevier.com/locate/ydbio

The role of floor plate contact in the elaboration of contralateral commissural projections within the embryonic mouse spinal cord

Stephanie R. Kadison [a,1], Fujio Murakami [b,2], Michael P. Matise [c,3], Zaven Kaprielian [a,*]

[a] *Albert Einstein College of Medicine, Department of Pathology and Dominick P. Purpura Department of Neuroscience, Kennedy Center, Rm. 624, 1410 Pelham Parkway South, Bronx, NY 10461, USA*

[b] *Laboratory of Neuroscience, Graduate School of Frontier Biosciences, Osaka University, Yamadaoka 1-3, Suita, Osaka 565-0871, Japan*

[c] *UMDNJ/Robert Wood Johnson Medical School Department of Neuroscience and Cell Biology, 675 Hoes Lane, Piscataway, NJ 08854, USA*

Received for publication 1 May 2006; revised 13 June 2006; accepted 13 June 2006
Available online 15 June 2006

Abstract

In vertebrate embryos, commissural axons extend toward and across the floor plate (FP), an intermediate target at the ventral midline (VM) of the spinal cord. After decussating, many commissural axons turn into the longitudinal plane and elaborate diverse projections. FP contact is thought to alter the responsiveness of these axons so that they can exit the FP and adopt new trajectories. However, a requirement for the FP in shaping contralateral commissural projections has not been established in higher vertebrates. Here we further analyze to what extent FP contact is necessary for the elaboration of decussated commissural projections both in cultured, FP-excised spinal cord preparations and in *gli2*-deficient mice, which lack a FP. In FP-lacking spinal cords, we observe a large number of appropriately projecting contralateral commissural projections in vivo and in vitro. Surprisingly, even though *gli2* mutants lack a FP, *slit1-3* mRNA and their receptors (Robo1/2) are expressed in a wild-type-like manner. In addition, blocking Robo-Slit interactions in FP-lacking spinal cord explants prevents commissural axons from leaving the VM and turning longitudinally. Thus, compared to FP contact, Slit-Robo interactions are more critical for driving commissural axons out of the VM and facilitating the elaboration of a subset of contralateral commissural projections.

Keywords: Commissural axon; Floor plate; Ventral midline; Contralateral; gli2; Slit; Robo; Rig-1; Spinal cord

Introduction

Growing axons often travel considerable distances along complex trajectories to reach their final targets. Specialized groups of cells known as intermediate targets subdivide these routes into smaller segments and provide axons with the guidance signals required for navigating the next leg of their journey. Spinal commissural axons follow a stereotypical circumferential trajectory to the floor plate (FP), an intermediate target located at the ventral midline (VM) of the embryonic vertebrate spinal cord (Kaprielian et al., 2001). After crossing through the FP, most commissural axons abruptly alter their direction of growth from the transverse to the longitudinal plane and elaborate a variety of contralateral projections (Kadison and Kaprielian, 2004; Nissen et al., 2005), but never re-cross the VM.

FP contact has been considered to be a prerequisite for this switch in pathfinding behavior (Brittis et al., 2002; Dodd et al., 1988; Kaprielian et al., 2001; Shirasaki and Murakami, 2001; Shirasaki et al., 1998). Accordingly, rodent commissural axons lose responsiveness to the chemoattractant, Netrin-1 (Shirasaki et al., 1998), and gain responsiveness to the repellents, Slit2 and Sema3B/3F (Zou et al., 2000) after encountering a FP, in vitro. Supporting these in vitro results, commissural axons in *slit1-3*-deficient mice erroneously stall at the VM or occasionally re-cross the FP. Furthermore, receptors for Slits (Robo proteins) are expressed exclusively on decussated commissural axons, consistent with their role in positioning longitudinal tracts in vivo (Long et al., 2004; Mambetisaeva et al., 2005; Sabatier et

* Corresponding author. Fax: +1 718 430 3758.
E-mail addresses: skadison@aecom.yu.edu (S.R. Kadison), murakami@fbs.osaka-u.ac.jp (F. Murakami), matisemp@umdnj.edu (M.P. Matise), kapriel@aecom.yu.edu (Z. Kaprielian).
[1] Fax: +1 718 430 3758.
[2] Fax: +81 6 6879 4659.
[3] Fax: +1 732 235 4029.

0012-1606/$ - see front matter © 2006 Elsevier Inc. All rights reserved.
doi:10.1016/j.ydbio.2006.06.022

al., 2004). Local guidance in the vicinity of the VM is mediated through the expression of contact-dependent cues located on the surface of FP cells, such as NrCAM, nectins, and ephrins (Imondi et al., 2000; Okabe et al., 2004; Stoeckli et al., 1997).

Previous analyses of FP-lacking mice at very early developmental stages have shown that most commissural axons reached the midline, but that few exited and/or extended longitudinal projections (Bovolenta and Dodd, 1991; Matise et al., 1999). In FP-lacking zebrafish mutants, however, nearly half of the Commissural Primary Ascending (CoPA) axons elaborate wild-type contralateral projections, suggesting that FP contact is not absolutely required for the proper guidance of decussated commissural axons in lower vertebrates (Bernhardt et al., 1992; Greenspoon et al., 1995; Hatta, 1992). A detailed analysis of post-crossing commissural projections in higher vertebrates has not been carried out, leaving open two key questions: can some rodent commissural axons elaborate appropriate contralateral projections without the experience of contacting FP cells, and if so, what guidance systems facilitate midline crossing and the formation of longitudinal tracts?

Consistent with previous observations in zebrafish embryos, we demonstrate here that a significant number of commissural axons elaborate wild-type-like contralateral projections in both cultured, FP-excised mouse spinal cord preparations and *gli2* null, FP-lacking mice. We further show that in *gli2* null embryos, decussated segments of commissural axons appropriately express Robo receptors and *slit* mRNA expression persists in the ventral ventricular zone. Supporting an active role for Robo-Slit signaling, even in the absence of FP contact, blocking Robo-Slit interactions in *gli2*$^{-/-}$ spinal cord explants prevents a significant number of commissural axons from leaving the VM and turning into the longitudinal plane. Our results suggest that a subset of commissural axons require Robo-Slit interactions, but not FP contact, in order to decussate and adopt appropriate contralateral projections.

Materials and methods

Mice

Timed pregnant CD1 mice were obtained from Charles River (Wilmington, MA). *Gli2* mutant mice were generated and genotyped as previously described (Mo et al., 1997). Nkx2.2 mutant mice were a kind gift from Thomas Jessell and were genotyped as previously described (Briscoe et al., 1999). Pregnant dams were killed by exposure to compressed carbon dioxide. Embryos were removed by cesarean section and immersed in phosphate-buffered saline (PBS; 150 mM Na_2HPO_4, 20 mM NaH_2PO_4, 150 mM NaCl, pH 7.4). Open book preparations were generated by slicing through the roof plate (RP) with a tungsten microneedle (Fine Science Tools; Foster City, CA), as previously described (Imondi and Kaprielian, 2001).

FP-excised and intact open book culture systems

To establish the FP-excised open book culture system, large (2.5 mm along the anterior–posterior (A–P) axis) open book preparations were dissected from thoracic and lumbar regions of E (embryonic stage) 12 mouse spinal cord as described above. Several of these open book preparations were fixed in 4% paraformaldehyde (PFA) and used for staging the extent of axonal growth at the beginning of the culture period. Importantly, focal application of DiI in these preparations revealed that very few of the resident commissural axons had reached the ipsilateral margin of the FP at this time. All FP tissue and immediately adjacent longitudinal fiber tracts were then removed (this was facilitated by the relative transparency of FP tissue) from the open book preparations that would ultimately be used to generate FP-excised explants. This was carried out through the use of a tungsten microneedle (Fine Science Tools; Foster City, CA) in ice-cold, Dulbecco's modified Eagle media (DMEM; Gibco-BRL; Carlsbad, CA) containing 10% fetal bovine serum (Gemini Bio-products), 1% penicillin/streptomycin/glutamine (Gibco-BRL; Carlsbad, CA), and 1% Bottenstein's N2 supplement (Gibco-BRL; Carlsbad, CA). These preparations were then trimmed to make one side shorter (~1 mm) than the other (~2.5 mm) and to promote tissue merging. Both "half open book" preparations were placed adjacent to one another on a 5.0-μm filter (Millipore) in a drop of media. The media were then aspirated off and the merged preparations were cultured in a three-dimensional collagen matrix as previously described (Imondi and Kaprielian, 2001). Intact open book preparations derived from thoracic levels of wild-type, heterozygous, or homozygous *gli2* spinal cords were cultured in a three-dimensional collagen matrix as described above.

In vitro perturbation experiments

Both merged and intact open book explants were cultured for 48 h in mock-conditioned media, media containing Fc recombinant protein (R&D Systems) or Robo1/Fc, after which time they were fixed in 2% PFA for a minimum of 2 h. FP-excised explants that were not sufficiently fused, identified by the appearance of a morphological gap or by the presence of axons that had turned at the border between the two pieces, were excluded from the analysis (9/34).

The cDNA construct used to generate Robo1/Fc was a kind gift from Marc Tessier-Lavigne (Genentech). Robo1/Fc-containing conditioned medium was generated as previously described (Sabatier et al., 2004). Robo1/Fc at an estimated concentration of 200 μg/ml and purified Fc at a concentration of 33 μg/ml were added to the various spinal cord preparations at the beginning of the culture period. The ability of Robo1/Fc to block Robo/Slit repulsion was tested in olfactory bulb explants co-cultured with Slit2-expressing 293 HEK cells as previously described, except that the tissue was dissected from E13.5 mouse brains (Li et al., 1999; Patel et al., 2001). In these experiments, axons were visualized with an anti-β-tubulin antibody (1:500; Supplemental Figs. 1A–C; mouse IgG; Sigma), and the transfection efficiency of *hSlit2* DNA was determined by labeling cell aggregates with an anti-myc antibody (1:200; Supplemental Figs. 1D–E; mouse IgG; Chemicon). Robo1/Fc successfully blocked the repulsion of olfactory bulb axons in these cultures, and a CY3 conjugated anti-human IgG Fc antibody (1:200; Chemicon) revealed the binding of Robo1 to Slit in these assays (Supplemental Fig. 1F).

Axon tracing

Crystal and focal application of 1,1′-dioctadecyl-3,3,3′,3′ tetramethylindocarbocyanine perchlorate (DiI; Molecular Probes) were performed in open book preparations as previously described (Kadison and Kaprielian, 2004). The DiI-labeled samples were placed in the dark in PBS for a maximum of 96 h to avoid retrograde labeling of cell bodies and/or overfilling of axons. DiI was always applied at a point halfway between the FP and roof plate, since this application site most consistently gives rise to all four classes of commissural axons (i.e., ILC, MLC, BLC, FTC). Similarly, we analyzed open book preparations from several different A–P levels, because each of the four commissural axon subtypes are present all along the A–P axis. In both the focal and crystal DiI analyses, every attempt was made to ensure that a uniform amount of DiI was applied to a given open book preparation. It should also be noted that there were no observable differences from spinal cord to spinal cord in either *gli2* mutant or wild-type embryos.

Immunohistochemistry

mAb 2H3 (mouse IgG; obtained from the Developmental Studies Hybridoma Bank) recognizes a 165-kDa protein in neurofilament-enriched cytoskeleton preparations (Dodd et al., 1988). mAb 4D7 (mouse IgM; obtained from the Developmental Studies Hybridoma Bank) recognizes the cell surface glycoprotein, TAG-1. Anti-L1 mAb (rat IgG; Chemicon) recognizes the L1

glycoprotein (Moos et al., 1988). The generation and characterization of anti-Robo1, -Robo2, and -Rig-1 polyclonal antibodies was previously described (Sabatier et al., 2004). mAb EphB recognizes rodent EphB1, EphB2, and EphB3 and was generated by immunizing mice with EphB1-Fc (A Jevince, SR Kadison, Z Kaprielian, unpublished observation). Whole-mount immunolabeling was performed essentially as described (Fazeli et al., 1997), except that an AP-conjugated goat anti-mouse IgG was used to detect mAb 2H3 binding. mAb 2H3, mAb 4D7, and anti-L1 immunolabeling of transverse cryosections derived from E12.5 and E13.5 mouse embryos was performed essentially as described (Schubert and Kaprielian, 2001), except that 1% Triton X-100 was added to the blocking solution used for L1 immunolabeling, a Cy2-conjugated goat anti-mouse IgG (Jackson Immunoresearch) was used to detect mAb 2H3 binding, a Cy2-conjugated goat anti-mouse IgM (Jackson Immunoresearch) was used to detect mAb 4D7 binding, and Cy2-conjugated goat anti-rat IgG (Jackson Immunoresearch) was used to detect anti-L1 binding. Cy3-conjugated goat anti-rabbit IgG (Jackson Immunoresearch) was used to detect anti-Robo1, anti-Robo2, and anti-Rig-1 binding.

In situ hybridization

The mouse *slit1*, *slit2*, and *slit3* cDNAs were generously provided by Yi Rao (Washington University School of Medicine). The mouse *netrin-1* cDNA was a kind gift from Marc Tessier-Lavigne (Genentech). The *shh* riboprobe was a kind gift from Jean Hebert (Albert Einstein College of Medicine). The *ephrin-B3* (Imondi et al., 2000) and *BEN* (Dillon et al., 2005) riboprobes were generated as previously described. Digoxigenin-labeled riboprobes were generated as previously described (Imondi and Kaprielian, 2001). In situ hybridization was performed as previously described (Kaprielian et al., 1995), except that anti-digoxigenin Fab fragments were pre-adsorbed with extracts derived from E12–E14 mouse embryos.

Microscopy and imaging

DiI labeling in open book explants was visualized through epifluorescent optics (Nikon Eclipse TE300; Nikon) using a Cy3/DiI optical filter (Chroma Technology). Black and white images of DiI labeling resulting from crystal applications and fluorescent antibody labeling were captured with a digital camera manufactured by Optronics, using compatible Magnafire software. The color merge function associated with Magnafire software was utilized for imaging Robo1 and L1 co-labeling.

Confocal images of DiI-labeled open book preparations (mainly focusing on the contralateral side of the FP/VM) and transverse sections were acquired on an Olympus Fluoview 500 microscope using a Cy3 optical filter. Slices were taken at a thickness of 2.5 μm and subsequently processed using Metamorph imaging software (Universal Imaging, Inc.). For the open book tricolor analyses, the most marginally/superficially located DiI-labeled axons located on the contralateral side of the FP/VM and contained within a 25-μm-thick slice of each open book were color-coded red. The contralaterally projecting axons contained within the next 25 μm of tissue were assigned the color green, and the remaining DiI-labeled axons, some of which were contralaterally projecting, and some of which were in the process of traversing the VM, were assigned the color blue (the thickness of this layer depended on the amount of DiI and the developmental stage and ranged from 2.5 to 50 μm). To ensure that the thickness of the axon-containing marginal zone did not differ significantly between homozygous and heterozygous *gli2* embryos, we measured the combined thickness of the red, green, and blue planes in both types of animals. This analysis revealed no significant difference between the thicknesses of the axon-containing zones in the two types of embryos. Most likely, this is due to the fact that our analyses were restricted to those axon segments located on the contralateral side of VM. Confocal imaging of large numbers of open books revealed that intermediate longitudinal commissural (ILC) axons were primarily located within the red layer. In contrast, medial longitudinal commissural (MLC) axons and bifurcating longitudinal commissural (BLC) axons were restricted to the green layer, and the blue layer contained mostly forked transverse commissural (FTC) axons (Fig. 3). Immunolabeling of open book preparations was visualized as previously described (Imondi et al., 2000). All color slides were scanned using an Agfa Duoscan flatbed scanner and imported into Photoshop 7.0. For color and black and white images, only the brightness and contrast were adjusted for increased visibility of axons. For some color slides, the color balance function was adjusted solely for color matching purposes.

Data analysis

For the quantification of pathfinding errors in the open book and FP-lacking explants cultured according to the conditions listed in the table in Fig. 8, cohorts (defined as axons emanating from a single DiI application) were scored based on the number of axons turning into the longitudinal direction and the presence or absence of stalled axons at the VM (see Fig. 8). Stalling was defined as stunted axonal growth in the immediate vicinity of the VM as compared to the significant growth observed in control (Fc or media) conditions. The statistical significance of the relationship between defective cohorts (cohorts displaying the phenotype of either "stalling" and/or "≤2 decussated longitudinal axons") and culture conditions ("media or Fc" and "Robo1/Fc") was determined using a Fisher's Exact Test; $p<0.05$ was taken to indicate significance.

For the quantification of pathfinding errors in *gli2* mouse embryos, the percentage of cohorts classified as "Perfect," "Slightly Imperfect," or "Aberrant" was determined by dividing the number of cohorts exhibiting one of these phenotypes by the total number of cohorts for a given genotype. It should be noted that the number of cohorts derived from each embryo was not always the same (see Table). A genotype-blind observer scored the cohorts, using examples of contralateral projection patterns illustrated in Fig. 1, Schematic A (see also Kadison and Kaprielian, 2004) as a wild-type baseline. "Perfect" cohorts included no axons that followed aberrant trajectories, "Slightly Imperfect" cohorts contained only one or two axons that followed abnormal trajectories, and "Aberrant" cohorts contained more than two axons extending along an atypical trajectory. Cohorts representative of those placed in each of these categories are illustrated in Fig. 2. Cohorts containing purely ipsilateral projections were eliminated from the analysis. The statistical significance of the relationship between genotype (heterozygous and homozygous) and category (Perfect, Slightly Imperfect, and Aberrant) was determined using a Fisher's Exact Test; $p < 0.05$ was taken to indicate significance. The trajectories (ILC, MLC, FTC, and BLC) shown in the Table were scored according to the criteria described in Kadison and Kaprielian (2004). For the immunohistochemical and in situ hybridization studies, a minimum of four cryosections per embryo was analyzed. For the cultured FP-lacking and open book explants, the number of explants analyzed is listed in the Results section of the text and in Fig. 8. In the experiments involving mutant mice, the number of cohorts and embryos for a given genotype is listed in the Table.

Results

Diversity of contralateral commissural projections in the embryonic mouse spinal cord

In E11.5 wild-type mouse embryos, dorsally positioned commissural neurons extend axons toward the FP, a key intermediate target located at the VM of the spinal cord. After crossing the VM, these early developing commissural axons execute an orthogonal turn and project alongside the FP in the rostral direction. We have recently shown that, by E12.5, axons emanating from both dorsally and ventrally located commissural neuron cell bodies elaborate one of at least four different types of contralateral projections (Fig. 1, Schematic A; Kadison and Kaprielian, 2004). Many of these decussated commissural axons extend away from the FP along an arcuate trajectory into intermediate regions of the spinal cord, where they ultimately make a second rostral turn into the longitudinal plane (ILC axons). However, a significant number of post-crossing axons project longitudinally, in the rostral direction, at a more medial position adjacent to the FP (MLC axons). A third group of commissural axons bifurcate and give rise to both rostral and

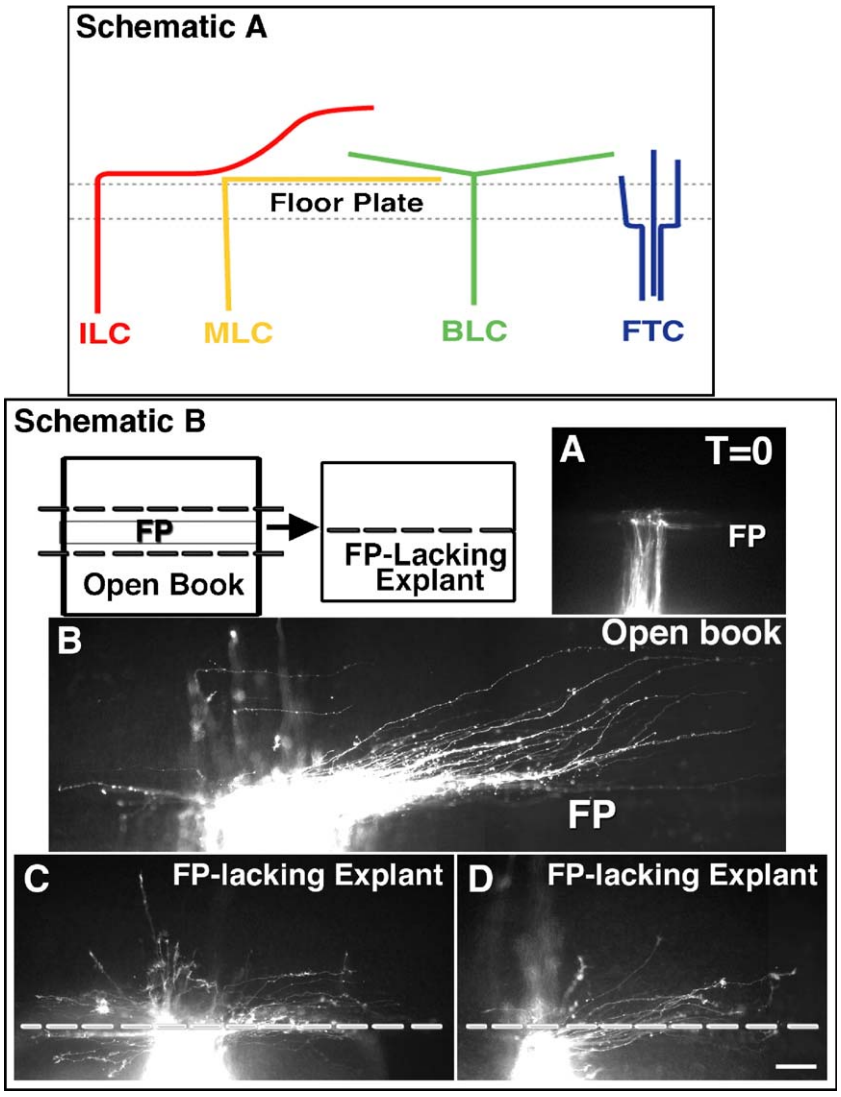

Fig. 1. Decussated commissural axons turn into the longitudinal plane, even in the absence of prior floor plate contact in vitro. (Schematic A) Diversity of contralateral commissural projections in the embryonic mouse spinal cord. Schematic depiction of four distinct commissural projections on the contralateral side of the floor plate (FP) in an open book preparation derived from an E12.5 or E13.5 wild-type mouse spinal cord. ILC, intermediate longitudinal commissural; MLC, medial longitudinal commissural; BLC, bifurcating longitudinal commissural; FTC, forked transverse commissural. See Results (or Kadison and Kaprielian, 2004) for details. (Schematic B) An open book preparation was dissected from an E12 mouse embryo as described in the Materials and methods. The floor plate (FP) and adjacent longitudinal tracts were then excised from the preparation and the two remaining pieces of the spinal cord placed next to each other ("FP-lacking Explant"). The FP-lacking explant was then grown in collagen for 48 h and the resident commissural axons were visualized with focal amounts of DiI. (A) A representative example of DiI-labeled axons in an open book preparation derived from the thoracic region of an E12 mouse spinal cord at the time of dissection (t=0). (B) An intact open book preparation cultured for 48 h in collagen displays wild-type-like contralateral projections. (C–D) Examples of DiI-labeled axons in representative FP-lacking explants. In these preparations, axons have crossed the ventral midline and turned into the longitudinal plane, even in the absence of a FP. While most of the labeled axons travel along wild-type-like ILC (Intermediate Longitudinal Commissural) trajectories, some caudally and transversely directed projections are also present in the FP-lacking explants. FP indicates the position of the floor plate and the dashed lines indicate the location of the ventral midline in FP-lacking explants. Scale bar, 100 μm.

caudal projections after crossing the VM (BLC axons). Forked transverse commissural (FTC) axons continue to project in the transverse plane after crossing the FP. When multiple FTC axons decussate, they form a forked-shaped projection.

Many commissural axons are capable of elaborating appropriate contralateral projections even in the absence of FP contact, in vitro

To assess the influence of FP contact on the proper elaboration of diverse contralateral commissural projections (Fig. 1, Schematic A), in vitro, we first excised the FP from E12 mouse open book preparations and merged the two sides of the spinal cord within a collagen gel (see Materials and methods). At this developmental stage, the majority of commissural axons in thoracic and lumbar regions of the spinal cord have yet to reach the VM. Notably, the dissection process necessarily severed the very few axons (see Materials and methods for more detail) that had contacted the ipsilateral margin of the FP. While it is conceivable that the growth cones associated with these axons could have retrogradely transported FP-derived guidance signals to more

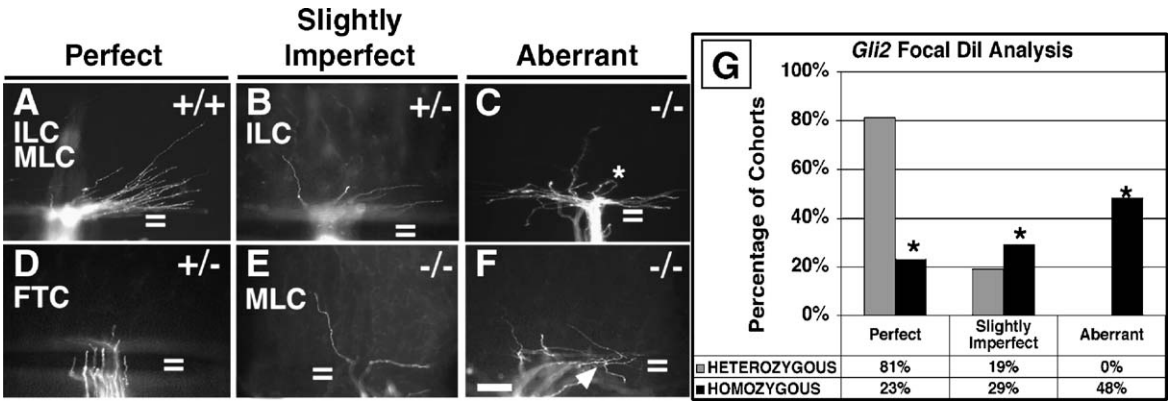

Fig. 2. In *gli2* homozygous mutants, a large number of commissural axons elaborate wild-type like projections. (A–F) Open book views of contralateral commissural projections visualized with focal applications of DiI in spinal cords derived from E12.5 and E13.5 *gli2* heterozygous, homozygous, and wild-type littermates. Each cohort (defined as axons emanating from a single application of DiI) was placed into one of the following three categories: "Perfect" (A, D), "Slightly Imperfect" (B, E), and "Aberrant" (C, F), according to the scoring criteria described in the Materials and methods. The "Perfect" and "Slightly Imperfect" categories include representative examples of ILC (A, B, E), FTC (D), and MLC (A) projections. In panel C, the asterisk denotes axon "looping," and in panel F, the arrowhead points to axonal clustering at the ventral midline. (G) Quantification of "Perfect," "Slightly Imperfect," and "Aberrant" cohorts in E12.5 and E13.5 *gli2* heterozygous (gray) and *gli2* homozygous (black) animals. Cohorts derived from *gli2* homozygous mutants were significantly more deviant than cohorts derived from heterozygous animals at both developmental stages. At the same time, roughly half of the *gli2* homozygous cohorts were classified as "Slightly Imperfect" and "Perfect," suggesting that a large subset of commissural axons in *gli2* heterozygotes are capable of elaborating appropriate contralateral trajectories. In panel G, the asterisk (*) indicates a p value < 0.05. An "=" indicates the location of the floor plate in *gli2* heterozygous or wild-type open book preparations or the ventral midline in *gli2* null preparations. ILC, intermediate longitudinal commissural; MLC, medial longitudinal commissural; FTC, forked transverse commissural. Scale bar, 100 μm.

proximal portions of the axon, which could subsequently influence the pathfinding of the newly formed growth cone at the cut edge, we consider this an unlikely possibility. We cultured the FP-lacking explants for 2 days (see Fig. 1, Schematic B and Materials and methods for details) and, subsequently, assessed the elaboration of contralateral commissural projections through the unilateral application of DiI. Surprisingly, a significant number of the axons that successfully crossed the midline in these cultured explants executed a rostral turn and elaborated wild-type-like longitudinal projections (19 out of 21 explants). These results were somewhat unexpected because a recent study demonstrated that rodent hindbrain-derived commissural axons require FP contact in order to execute a stereotyped orthogonal turn on the contralateral side of the VM in vitro (Shirasaki and Murakami, 2001). A bona fide difference between spinal and hindbrain commissural neurons/axons (or differences in the configuration of the explant systems) might account for these apparent inconsistencies. More specifically, in our FP-lacking cultured explants, the majority of contralateral projections we examined displayed ILC (17/21 explants) and MLC axons (18/21 explants). In addition to rostrally directed axons, we also frequently observed FTC (14/21 explants) and BLC (10/21 explants) projections that closely resembled their wild-type counterparts (Fig. 1C). Notably, we observed an unusually high frequency of FTC projections, which may be due to the fact that, even in intact (FP-containing) cultured open book explants, we typically observe an exaggerated number of transverse projections/FTC axons when compared to open book preparations derived from a comparable developmental stage in vivo. Taken together, these observations show that, at least in vitro, commissural axons that never contact a FP are capable of crossing the VM and adopting appropriate contralateral trajectories.

Commissural axons exhibit both aberrant and wild-type-like contralateral projections in the gli2 homozygous mutant spinal cord

To determine whether FP contact is required for the proper elaboration of contralateral commissural projections in vivo, we analyzed *gli2* mouse mutant spinal cords. The *gli2* mutant is generally regarded as the best in vivo mammalian model for studying the role of the FP in axonal pathfinding. This is because *gli2* null embryos lack FP cells (Supplemental Fig. 2) but do not exhibit overt defects in the patterning of the ventral spinal cord. However, these animals do possess a reduced number of V3 interneurons (Dillon et al., 2005; Ding et al., 1998; Matise et al., 1998, 1999).

In previous analyses of E11–E11.5 FP-lacking, *gli2*$^{-/-}$ mouse embryos, many spinal commissural axons were observed to cluster at the VM and failed to make the transition from circumferential to longitudinal growth (Matise et al., 1999). The small number of axons that appeared to successfully execute a turn into the longitudinal plane inappropriately grew within the immediate vicinity of the VM, a region normally occupied by the FP. In addition, many longitudinal projections were directed posteriorly, even though caudal projections in wild-type animals are rare at these relatively early ages (see above; Matise et al., 1999). We reasoned that, by examining later stages of spinal cord development in these animals, it would be possible to determine whether the elaboration of appropriate contralateral commissural projections is reliant on prior FP contact. Towards this end, we used focal applications of DiI to analyze contralateral commissural projections in open book preparations

derived from the spinal cords of E12.5 and E13.5 heterozygous and homozygous *gli2* embryos.

Consistent with previous a previous study that focussed on early stages (E11.5–12) of commissural axon growth (Matise et al., 1999), we found that some axons clustered within the immediate vicinity of the VM in *gli2* null embryos at E12.5 and E13.5 (Fig. 2F; arrowhead). In addition, a subset of axons executed loops (Fig. 2C; asterisk) or exhibited highly disorganized contralateral projections (Figs. 2C, F). Notably, these types of pathfinding defects were never observed in wild-type (Fig. 2A and data not shown) or heterozygous littermates (which contain a FP) at these development stages (Figs. 2B, D and data not shown). In order to quantify the phenotypes observed in *gli2* mice, each cohort, defined as the group of axons labeled by a single application of DiI, was categorized as either "Perfect," "Slightly Imperfect," or "Aberrant" (see Materials and methods for details). This quantification revealed that nearly half (48%) of the cohorts derived from *gli2* null spinal cords displayed "Aberrant" contralateral pathfinding behavior. Notably, at both E12.5 and E13.5, this category contained solely *gli2*$^{-/-}$ cohorts, suggesting that prior FP contact is required for the proper guidance of a significant proportion of decussated cohorts (Fig. 2G).

Consistent with our observations in the FP-lacking culture system described above, many *gli2*$^{-/-}$ cohorts contained only one to two (Slightly Imperfect; 29%) or zero (Perfect; 23%) axons that followed aberrant contralateral trajectories. Thus, slightly more than half (52%) of the cohorts labeled in *gli2* homozygous mutants displayed virtually error-free projection patterns on the contralateral side of the VM. Notably, each of these wild-type-like cohorts contained multiple axons that followed MLC, ILC, BLC or FTC projections, which closely resembled those elaborated by axons in their heterozygous littermates at both developmental stages. The significant number of wild-type-like trajectories observed in the *gli2* null embryos suggests that some commissural axons are not reliant on FP contact for proper pathfinding on the contralateral side of the VM. To determine whether each of the distinct contralateral projections is present in the *gli2* null spinal cord, we assessed the frequency of MLC, ILC, BLC, or FTC projections in homozygous, as compared to heterozygous, animals (Table 1).

Table 1
Trajectory types observed in heterozygous versus homozygous *gli2* mice [a]

Genotype	MLC	ILC	BLC	FTC	Total no. of trajectories [b]	No. of cohorts [c]	No. of embryos
gli2$^{+/-}$	16	40	12	13	81	42	25
gli2$^{-/-}$	15	14	4	4	37	44	11

[a] Focal amounts of Dil were applied to a position halfway between the roof plate and floor plate in open book preparations derived from all anterior–posterior levels of E12.5 and E13.5 gli2 homozygous and heterozygous spinal cords.

[b] A trajectory refers to one of the four distinct contralateral projections (MLC, ILC, BLC, and FTC) observed in wild-type embryonic rodent spinal cord.

[c] Cohorts are defined as a group axons emanating from a single Dil application. The number of trajectories observed in cohorts derived from *gil2* mutants was fewer because many of these cohorts contained aberrant axons that could not be classified as one of the four trajectories.

The presence of all four projection patterns in homozygous *gli2* animals suggests that, even without the prior experience of contacting FP cells, a number of commissural axons are capable of elaborating each of the four distinct contralateral trajectories we previously described in wild-type animals (Table 1; Kadison and Kaprielian, 2004).

To obtain a more global view of contralateral projections in the *gli2*$^{-/-}$ mouse spinal cord, we applied large crystals of DiI to open book preparations derived from E12.5 and E13.5 animals. Due to the copious number of axons labeled by crystal applications of DiI, wild-type-like contralateral commissural axons were present in nearly every cohort at either embryonic age. Whereas some of the axons in these cohorts were clearly confined to the VM, a significant number had turned into the longitudinal plane and extended within intermediate regions of the spinal cord (see Figs. 4E, F). These findings are generally consistent with the results of the focal DiI analyses and suggest that while some commissural axons make contralateral pathfinding errors, a significant number are capable of extending along wild-type-like contralateral trajectories by E12.5 and E13.5, even if they have never encountered a FP.

We also used confocal microscopy to more carefully examine the spatial organization of contralateral commissural projections in DiI-labeled open book preparations derived from both wild-type and *gli2* mutant animals. Specifically, we first asked whether the various classes of contralateral commissural projections are normally segregated to particular layers of the *z*-axis. In this approach, decussated axons residing in the most marginal layer were designated red (25 μm), those in the adjacent layer were designated green (25 μm), and post-crossing axons contained within the most ventricular layer were designated blue (variable thickness depending on amount of DiI and developmental stage; see Fig. 3 and Materials and methods). Using this color-coding strategy, we found that, in E12.5 and E13.5 wild-type and heterozygous embryos, nearly all of the ILC projections were contained within the most marginal layer. In addition, most MLC and BLC axons were located in the green/more ventricular layer, and essentially all of the FTC axons resided within the most ventricular blue layer (Fig. 3). Some commissural axon subtypes were clearly disrupted in *gli2*$^{-/-}$ mutants. For example, in mutant embryos, a number of "green" MLC axons were observed to course within the VM and elaborate disorganized contralateral projections (Fig. 4G) and there were noticeably fewer "blue" FTC projections (7/18 cohorts; Fig. 4H). Nevertheless, red, wild-type-like ILC axons were confined to the most marginal layer of the *gli2* null spinal cord, just as they are in heterozygous littermates (17/18 cohorts; Fig. 4F). In addition, MLC and some caudally projecting axons (that presumably represent the caudal projections of BLC axons) were observed within the green layer in most *gli2* homozygous spinal cords and resembled their wild-type counterparts (MLC: 18/18 cohorts; BLC: 16/18 cohorts; Fig. 4G). Taken together, these particular observations suggest that the elaboration of each of the four main contralateral commissural projections is minimally disrupted in *gli2* null embryos.

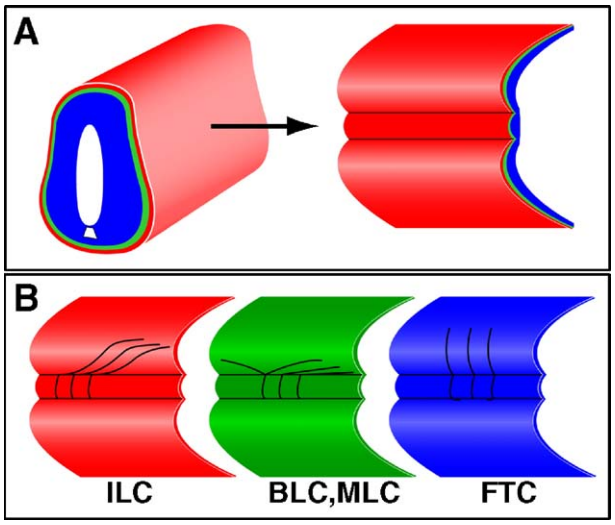

Fig. 3. Distinct contralateral commissural projections occupy separate layers of the marginal zone. (A) Schematic representation of the spinal cord in transverse and open book views. The red layer contains decussated commissural axons traveling within the most superficial portion of the marginal zone (25 μm) and the green layer contains axons traveling within the adjacent 25 μm of tissue. Axons traveling within the most ventricular layer of the marginal zone (variable thickness depending on amount of DiI and developmental stage) are contained within the blue layer. (B) After applying a DiI crystal to the ipsilateral side of an open book preparation, commissural projections on the contralateral side of the ventral midline were visualized by confocal microscopy. Using the color coding strategy in panel A, ILC, FTC, BLC, and MLC axons occupied distinct layers of the marginal zone. ILC, intermediate longitudinal commissural; MLC, medial longitudinal commissural; BLC, bifurcating longitudinal commissural; FTC, forked transverse commissural.

As noted previously, *gli2*$^{-/-}$ mouse embryos lack FP cells and display a reduction in the number of V3 interneurons (Briscoe et al., 1999). Since V3 interneurons are selectively absent in *nkx2.2* mutant mice, we analyzed commissural axon pathfinding in these particular animals to ensure that the commissural axon phenotype we observed in *gli2* mutant embryos was specifically attributable to the loss of FP cells. Accordingly, we examined contralateral commissural projections in open book preparations derived from E12.5 and E13.5 *nkx2.2* null embryos (Briscoe et al., 1999). Unilateral application of DiI revealed only wild-type-like contralateral commissural projections in spinal cords lacking *nkx2.2* (data not shown).

Commissural axons in the gli2 null spinal cord maintain normal cell surface protein expression patterns

In wild-type rodent embryos, pre-crossing segments of commissural axons express the Ig domain-containing cell surface protein, TAG-1, whereas the post-crossing segments of these axons are thought to express the L1 glycoprotein (Dodd et al., 1988) and EphB receptors (Imondi et al., 2000; Jevince et al., 2006). The prevailing view has been that the so-called 'TAG-1 to L1 switch' and the presumed upregulation of EphB expression are, at least in part, induced by contact-dependent interactions between commissural axons and FP cells. As previously reported, TAG-1-positive axons projected to the VM in a defasciculated manner in E11.5 *gli2* null embryos, presumably due to the absence of FP-derived Sonic Hedgehog (Shh; see Supplemental Figs. 2A, B) (Charron et al., 2003). By E12.5, TAG-1 expression was appropriately restricted to pre-crossing commissural axons in both *gli2* homozygous and heterozygous animals (Supplemental Figs. 3A, B; Matise et al., 1999).

To determine whether decussated portions of commissural axons not only downregulate TAG-1 expression but also upregulate L1 and EphB expression, in *gli2* homozygous mutants, we labeled transverse sections taken from E12.5 and E13.5 *gli2* null spinal cords with monoclonal antibodies specific for TAG-1, L1 or EphB proteins. In contrast to TAG-1 staining, which is primarily restricted to pre-crossing segments of commissural axons (Supplemental Figs. 3A, B), anti-L1 labels longitudinally oriented commissural axons, as well as some axons that erroneously project toward the ventral ventricular zone in E12.5 *gli2* null embryos (Fig. 5B1, arrowhead). By E13.5, L1-positive axons in *gli2* homozygous embryos avoided the ventral ventricular zone and formed organized longitudinal tracts within the marginal zone, similar to what we observed in heterozygous littermates (compare Figs. 5G, H). At E13.5, anti-EphB also labeled longitudinal tracts, including longitudinally oriented

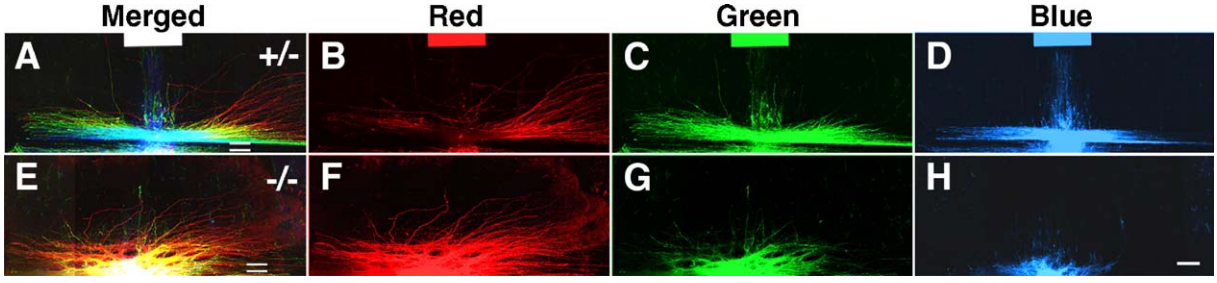

Fig. 4. At E13.5, wild-type-like longitudinally-oriented axons are present on the contralateral side of the ventral midline in *gli2*$^{-/-}$ mice. (A–H) Open book views of contralateral commissural projections visualized with applications of large DiI crystals in E13.5 *gli2* heterozygous and homozygous mice. The "Merged" view includes red-, green-, and blue-colored axons. The single color images ("Red," "Green," and "Blue") are included to show the particular subsets of decussated commissural axon populations that are contained within each layer of the marginal zone (see Fig. 3 and the Results). The red plane contains primarily ILC axons (B, F), both BLC and MLC projections are present in the green plane (C, G), and the blue plane is mainly composed of FTC axons (D, H). Notably, the red plane highlights commissural axons in *gli2*$^{-/-}$ mice that successfully decussate and execute ILC-like projections that closely resemble those present in heterozygous littermates (compare panel B to panel F). ILC, intermediate longitudinal commissural; MLC, medial longitudinal commissural; BLC, bifurcating longitudinal commissural; FTC, forked transverse commissural. An "=" indicates the location of the floor plate in a *gli2* heterozygous open book preparation or the ventral midline in a *gli2* homozygous preparation. Scale bar, 100 μm.

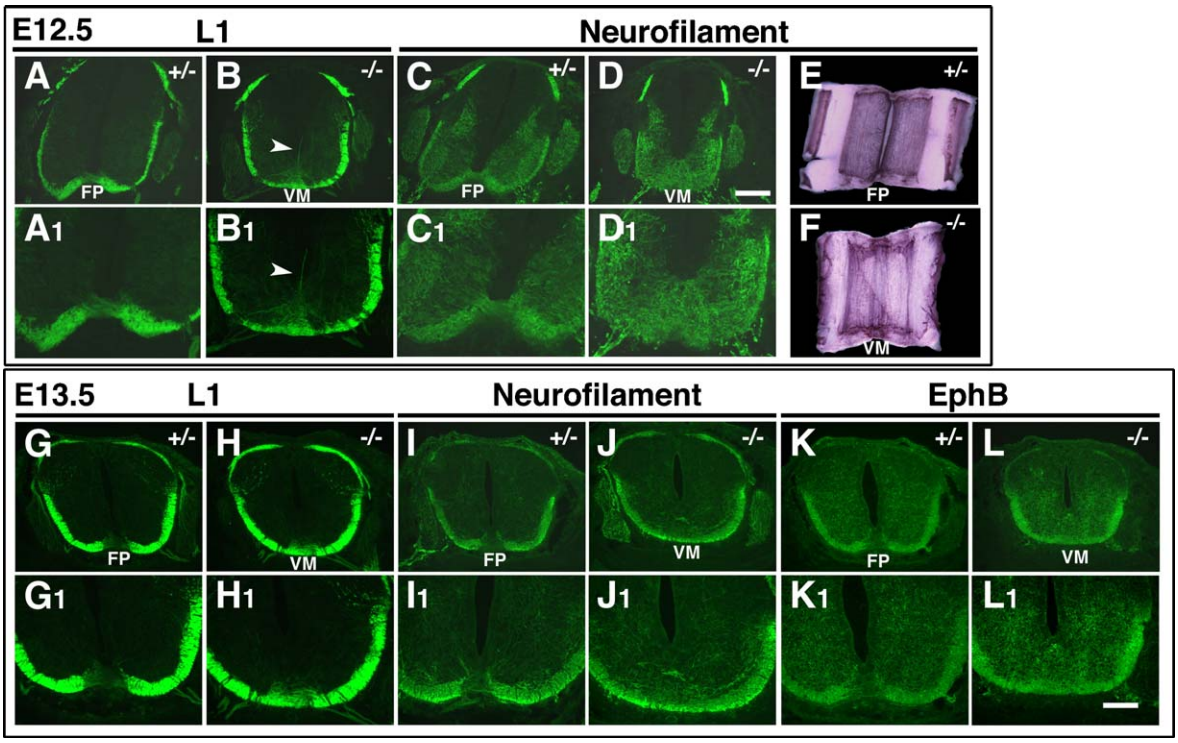

Fig. 5. L1 protein is expressed almost exclusively on longitudinal tracts, which remain highly organized in *gli2* homozygotes. Transverse cryosections derived from E12.5 (A–D) and E13.5 (G–L) *gli2* heterozygous and homozygous embryos and open book preparations derived from E12.5 (E–F) *gli2* heterozygous and homozygous spinal cords. (A1–D1, G1–L1) High magnification (2×) views of the ventral midline region in panels A–D and G–L. Anti-L1 labels longitudinally oriented commissural axons (A, B, G, H), anti-neurofilament is a pan-axonal marker (C–F, I, J) and anti-EphB labels longitudinal tracts, which are mainly composed of commissural axons (K, L). At E12.5, in *gli2* homozygous embryos, anti-L1 labels longitudinally oriented commissural axons, as well as some axons that erroneously project toward the ventral ventricular zone (arrowhead in B1). (H) By E13.5, however, commissural axons in the *gli2* homozygote appropriately avoid the ventricular zone and form organized longitudinal fascicles within the marginal zone. (E–F) Anti-neurofilament labeling reveals the overall organization of longitudinal tracts in an open book preparation derived from an E12.5 *gli2*$^{-/-}$ mutant. Note that axons occupy the ventral midline in the *gli2* homozygous mutant, whereas this area is devoid of axonal tracts in the *gli2* heterozygous littermates. FP indicates the location of the floor plate in a *gli2* heterozygote and VM denotes the ventral midline in a *gli2* homozygous mutant. Scale bar, 100 μm.

commissural axons, in *gli2* heterozygous and homozygous littermates (Figs. 5K, L). To assess the overall organization of axonal tracts, we labeled both transverse cryosections and open book preparations derived from E12.5 and E13.5 homozygous and heterozygous *gli2* embryos with the pan-axonal marker, anti-neurofilament (NF), which recognizes a 165-kDa protein in NF-enriched cytoskeleton preparations (Dodd et al., 1988). This marker revealed the presence of organized longitudinal fascicles, even within the VM, a region typically devoid of axonal tracts, in an open book preparation derived from an E12.5 *gli2* null spinal cord (Figs. 5E, F). Based on our DiI analyses of *gli2* null embryos, a subset of these longitudinal projections are presumably composed of decussated commissural axons. Taken together, the results of these immunohistochemical analyses suggest that FP contact is not required for the presumed upregulation of L1 and EphB on the contralateral segments of a significant number of commissural axons.

Slit1-3 mRNA is expressed in the vicinity of the VM in gli2$^{-/-}$ *mutants*

After contacting the FP, commissural axons gain responsiveness to the midline repellents Slits and Semaphorins in vitro and, presumably, in vivo (Long et al., 2004; Stein and Tessier-Lavigne, 2001; Zou et al., 2000). This change in responsiveness is thought to expel commissural axons out of the VM and "squeeze" them into longitudinal tracts (Zou et al., 2000). As described above, some commissural axons ultimately turn into the longitudinal plane and elaborate wild-type-like contralateral projections even in the absence of a FP in vivo and in vitro. This raised the possibility that decussated commissural axons are capable of altering their responsiveness to VM-associated repellent guidance cues, without ever having encountered a FP. As a first step toward testing this hypothesis, we asked whether Slits are still expressed in the vicinity of the VM in *gli2* null embryos by performing in situ hybridization using digoxigenin-labeled *slit1-3* probes on transverse cryosections derived from E12.5 and E13.5 *gli2* heterozygous and homozygous littermates (Fig. 6). In *gli2* heterozygotes, as has previously been described in wild-type animals, *slit1* and *slit2* mRNA was expressed at high levels in the FP (Figs. 6A, C, E, G). Unexpectedly, we found that *slit1* and *slit2* mRNA is expressed within the ventral ventricular zone of *gli2* homozygous mutants, despite the absence of a FP (Figs. 6B, D, F, H). Interestingly, *slits* are normally expressed within this region of the VM (as well as by FP cells) in heterozygous and wild-type embryos. Notably, *slit*

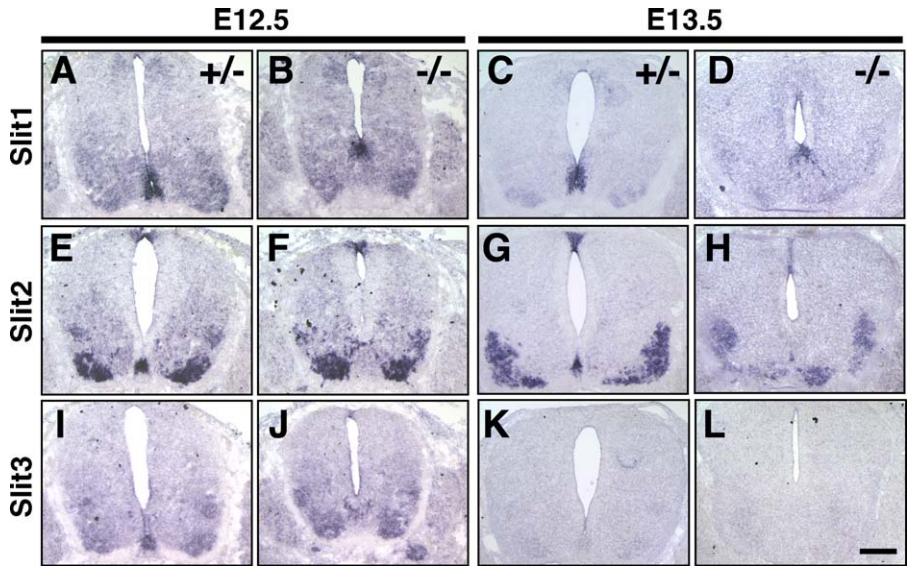

Fig. 6. *Slit* mRNA is expressed within the ventral ventricular zone of *gli2*$^{-/-}$ mutant spinal cords. In situ hybridization with digoxigenin-labeled *slit1* (A–D), *slit2* (E–H), and *slit3* (I–L) probes was performed on transverse cryosections derived from thoracic levels of E12.5 and E13.5 *gli2* heterozygous and homozygous littermates. (A–D) In *gli2* heterozygous and homozygous littermates, *slit1* mRNA is expressed in the vicinity of the ventral ventricular zone and in motoneurons. *slit2* (E–H) and *slit3* (I–L) mRNA are localized to motoneurons and the roof plate in *gli2* homozygous mutants, and are also expressed at high levels by floor plate cells in *gli2* heterozygotes. *Slit2* and *slit3* are expressed in the vicinity of the ventral ventricular zone in *gli2* homozygous mutants but at lower levels than *slit1*. (K–L) At E13.5, *slit1* and *slit2* mRNA expression levels are maintained, whereas *slit3* mRNA expression is significantly diminished in both homozygous and heterozygous mutants. Scale bar, 100 μm.

and *netrin-1* mRNA expression patterns display significant overlap in the mutant spinal cord (Supplemental Figs. 2G, H; see also Matise et al., 1999). Similar to what we observed in heterozygous littermates, *slit1-3* mRNA was also expressed by motoneurons and within the roof plate in *gli2* null embryos (Fig. 6, except *slit3* at E13.5). In addition, *slit3* mRNA expression resembled the distribution of *slit1* and *slit2* at E12.5, but the overall level of *slit3* mRNA expression diminished by E13.5 in both homozygous and heterozygous embryos (Figs. 6I–L).

In gli2$^{-/-}$ *mutants, Robo1 and Robo2 are appropriately restricted to longitudinal tracts, whereas Rig-1 expression is inappropriately maintained beyond the VM*

The Slit receptors, Robo1, Robo2, and Rig-1 (Robo3) have previously been shown to play critical roles in commissural axon pathfinding (Brose et al., 1999; Jen et al., 2004; Kidd et al., 1998, 1999; Long et al., 2004; Marillat et al., 2004; Rajagopalan et al., 2000; Sabatier et al., 2004). Robo1 and Robo2 are required for the formation of contralateral longitudinal fascicles located at various dorsoventral positions (Long et al., 2004; Rajagopalan et al., 2000; Simpson et al., 2000). Consistent with this role, Robo2 protein is specifically expressed on lateral funiculi, whereas Robo1 protein is localized to both ventral and lateral funiculi in the wild-type spinal cord (Long et al., 2004; Mambetisaeva et al., 2005). In contrast to Robo1 and Robo2, Rig-1 expression is normally high on pre-crossing commissural axons and downregulated after these axons cross through the ventral commissure. This expression pattern reflects a critical role for Rig-1 in the decision to cross the midline of the CNS (Jen et al., 2004; Marillat et al., 2004; Sabatier et al., 2004).

To determine whether Robo receptor expression was appropriately regulated in *gli2* homozygous embryos, we labeled transverse cryosections derived from homozygous and heterozygous littermates with antibodies specific for Robo1, Robo2, or Rig-1. Robo1 protein expression was localized to ventral and lateral funiculi (Figs. 7A–D), whereas Robo2 selectively labeled lateral funiculi (Figs. 7E–H). To compare the trajectories of axons expressing Robo1 and those expressing the more promiscuous axonal marker, L1, we double-labeled transverse cryosections derived from E12.5 and E13.5 *gli2* homozygous and heterozygous embryos with anti-Robo1 and anti-L1 (Figs. 7I–L). At E12.5, L1-positive axons, but not Robo1-positive axons, aberrantly projected toward the ventral ventricular zone (Fig. 7J, arrowhead and see Fig. 5B1, arrowhead). By E13.5, however, L1-positive axons also appropriately turned into the longitudinal axis in the *gli2* homozygous mutant (Fig. 7L). Thus, axons that express Robo1 appear to “escape” the VM and form longitudinal tracts, just as they do in wild-type animals, presumably by gaining responsiveness to ventral ventricular zone-associated Slits (see Fig. 6). It must be noted, however, that a subset of Robo- and L1-positive axons turn and extend within the VM, at a position where the FP no longer separates the two sides of the spinal cord (Figs. 7J, L).

Although Robo1 and Robo2 were appropriately regulated in the *gli2* homozygous mutant, this was not the case for Rig-1 (Supplemental Figs. 3C, D). In *gli2* homozygotes, Rig-1 protein expression persists on commissural axons even after they reach the VM and turn into the longitudinal plane,

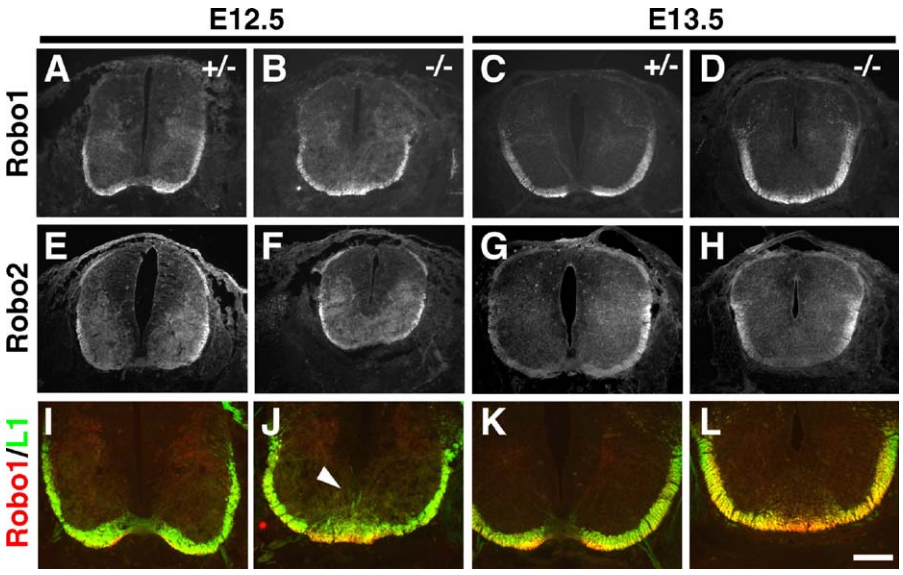

Fig. 7. Robo1 and Robo2 protein are appropriately localized to longitudinal tracts in *gli2* homozygous mutants. Transverse cryosections derived from E12.5 (A, B, E, F, I, J) and E13.5 (C, D, G, H, K, L) heterozygous and homozygous *gli2* embryos. (I–L) High magnification (2×) views of the ventral midline region depicted in panels A–D. (A–D) Robo1 protein expression is localized to ventral *and* lateral funiculi in *gli2* homozygous mutants, just as it is in *gli2* heterozygous littermates. (E–H) Anti-Robo2, in contrast, selectively labels only *lateral* funiculi in cryosections derived from *gli2* heterozygous and homozygous embryos. (I–L) Double labeling with anti-LI and anti-Robo1 reveals differences between the trajectories of Robo1-positive axons (red) and L1-positive axons (green) in heterozygous and homozygous *gli2* embryos. Yellow reflects overlapping L1 and Robo1 protein expression. At E12.5, L1-positive axons, but *not* Robo1-positive axons, aberrantly extend toward the ventral ventricular zone (arrowhead in panel J). By E13.5 (L) however, both L1-positive *and* Robo1-positive axons have appropriately turned into the longitudinal plane in *gli2* homozygous mutant embryos. Scale bar, 100 μm.

although it is not clear whether these axons have successfully crossed the VM (Supplemental Fig. 3D). This particular observation suggests that Rig-1 expression may identify a subclass of commissural axons that is particularly dependent on FP contact for subsequent pathfinding decisions. Taken together, these results suggest that the proper regulation of Rig-1, but not Robo1 and Robo2, expression requires FP contact.

Blocking Robo-Slit interactions prevents commissural axons from exiting the VM in FP-lacking explants

Previous studies have shown that interfering with Robo-Slit interactions results in axonal stalling at the VM and a reduced thickness of decussated longitudinal tracts in ovo (Mambetisaeva et al., 2005), and in vivo (Long et al., 2004). To indirectly determine whether commissural axons require FP contact in order to become responsive to Slit and subsequently leave the VM, we assessed the consequences of blocking Robo-Slit interactions in open book explants derived from E12 *gli2* null embryos. Specifically, intact open book preparations derived from E12 heterozygous or homozygous *gli2* littermates (see Fig. 8, Schematic and Materials and methods) were cultured in the presence of mock-conditioned media, Fc, or Robo1/Fc. After 2 days in culture, we visualized commissural axon projection patterns by unilaterally applying focal amounts of DiI to each explant. In heterozygous explants cultured in the presence of media or Fc, all of the cohorts displayed more than two axons projecting along the longitudinal plane (6/6; Fig. 8C). In contrast, when heterozygous explants were cultured in the presence of Robo1/Fc, less than half (4/10) of the cohorts displayed more than two decussated axons that had successfully turned into the longitudinal plane (4/10; Fig. 8E). In the *gli2* homozygous embryo-derived explants cultured in the presence of Robo1/Fc, the resident cohorts rarely (2/9) contained more than two axons that decussated and turned into longitudinal tracts, as compared to control conditions (6/6; compare Fig. 8D to Figs. 8F and G). The most striking phenotype observed in both heterozygous and homozygous explants treated with Robo1/Fc (6/10 and 6/9 cohorts, respectively) was axon stalling at the VM (arrowhead in Fig. 8G and data not shown). Importantly, similar midline-associated and turning defects were observed in FP-excised open book explants that were derived from wild-type embryos (see Fig. 1, Schematic B) and grown in the presence of Robo1/Fc (6/8 cohorts exhibited defects; Fig. 8H). Together, these in vitro observations are consistent with the possibility that some commissural axons can gain responsiveness to midline-associated Slit and leave the immediate vicinity of the VM even if they never encounter a FP.

Discussion

Spinal commissural axons extend along a simple, circumferential path toward the FP. After crossing the VM, most of these axons turn into the longitudinal plane and elaborate complex trajectories (Kadison and Kaprielian, 2004). Although FP contact is thought to alter the responsiveness of these axons

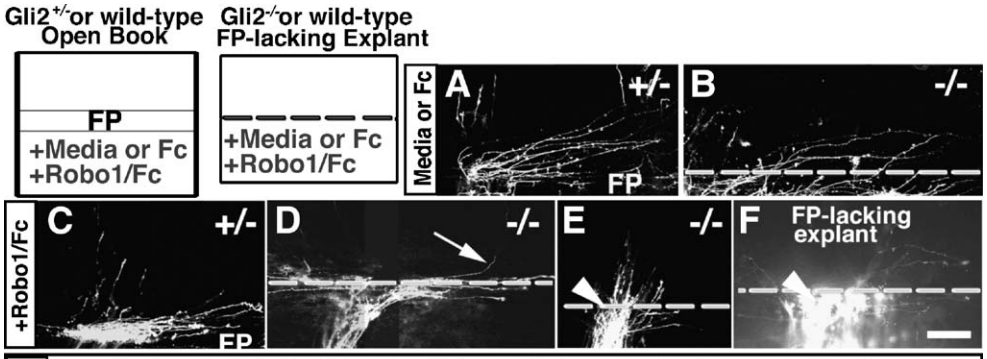

G Quantification of pathfinding defects in *gli2* $^{+/-}$ and *gli2* $^{-/-}$ open book cultures and FP-lacking explants

Type of Explant	Culture Conditions	Cohorts Exhibiting Stalling	Cohorts containing ≤2 Decussated Longitudinal Axons	Cohorts Exhibiting no Defects	Total Number of Cohorts[1]
gli2 $^{+/-}$ open book	media or Fc	0	0	6	6
gli2 $^{-/-}$ open book	media or Fc	1	0	5	6
gli2 $^{+/-}$ open book	Robo1/Fc	6*	6*	4	10
gli2 $^{-/-}$ open book	Robo1/Fc	6*	7*	2	9
FP-lacking explant	media or Fc	2	1	19	21
FP-lacking explant	Robo1/Fc	3**	3**	2	8

[1]In some cases, a single cohort was placed into multiple categories, therefore, in these instances, the sum of cohorts exceeded the total number of cohorts

*Indicates a statistically significant relationship between the culture condition and cohorts containing pathfinding defects ("stalling" and/or "≤2 decussated longitudinal axons"); $P < 0.05$, Fisher's exact test.

**P value < 0.001; Fisher's exact test.

Fig. 8. Commissural axons fail to leave the immediate vicinity of the ventral midline when Robo/Slit interactions are blocked in cultured explants, which lack a floor plate. (Schematic) Intact open books derived from heterozygous or homozygous *gli2* mouse embryos or FP-lacking explants derived from wild-type embryos (see Fig. 1 and Materials and methods) were cultured for 48 h in the presence of "Fc" (Fc-containing media), "Media" (mock-conditioned media), or Robo1/Fc. (A–B) Representative examples of DiI labeling in intact open book and FP-lacking explants cultured under control (Fc or media) conditions. Open book preparations derived from *gli2* heterozygous (A) and homozygous (B) spinal cords contain axons that decussate and extend significant distances along the longitudinal axis when cultured in control conditions (mock-conditioned media, in both of these cases). (C–F) Representative examples of DiI labeling in intact open book and FP-lacking explants cultured in the presence of Robo1/Fc. (C) In open book preparations derived from *gli2* heterozygotes, axons cross the FP and turn into the longitudinal plane roughly half of the time (4/10 cohorts), which was significantly less than those grown under control conditions (6/6 cohorts). (D–E) In explants derived from *gli2* homozygous embryos cultured in the presence of Robo1/Fc, the resident cohorts rarely (2/9) contained more than two axons that crossed the VM and turned into the longitudinal plane, as compared to control conditions (5/6 cohorts). In these same conditions, axon stalling at the ventral midline was the most frequently observed phenotype (6/9 cohorts; arrowhead). (F) DiI-labeled axons in this merged, FP-lacking explant stalled at the ventral midline (arrowhead), as do most labeled cohorts in *gli2*$^{-/-}$ mutant-derived open book explants grown in the presence of Robo1/Fc. The arrow points to a retrogradely labeled axon that has turned ipsilaterally prior to crossing the ventral midline in panel D. Arrowheads mark axons that stall at the ventral midline in panels E and F. Dashed lines indicate the location of the ventral midline in merged explants and *gli2* homozygous open book explants, and FP indicates the position of the floor plate in the *gli2* heterozygous preparations. All panels except panel F represent confocal micrographs. Scale bar, 100 μm. (G) Quantification of defects observed in the Robo-Slit perturbation experiments. In *gli2* homozygous, heterozygous, or FP-lacking explants cultured in the presence of Robo1/Fc, a significantly higher number of defects were observed, as compared to control conditions (Fc and media). Defects were classified into two categories (which were not always mutually exclusive): cohorts exhibiting either stalling behavior at the midline or cohorts containing less than two decussated longitudinal axons. These results suggest that Robo-Slit interactions, but not FP contact, are required for exiting the ventral midline and forming decussated longitudinal tracts.

to midline-associated cues so that they can adopt new post-crossing trajectories, this has not been established in the rodent spinal cord. Here we demonstrate that commissural axons are capable of elaborating appropriate contralateral projections in cultured FP-lacking embryonic mouse spinal cord explants. Consistent with this observation, approximately half of the commissural axon-containing cohorts examined travel along wild-type-like trajectories on the contralateral side of the VM in *gli2* null, FP-deficient mouse embryos. We also show that *slit1-3* mRNA and Robo protein are expressed in spinal cords derived from *gli2* homozygous embryos in a pattern resembling that observed in heterozygous littermates. In addition, blocking Robo-Slit interactions in FP-lacking explants inhibits the majority of commissural axons from decussating and turning into the longitudinal plane. These results suggest that spinal commissural axons are capable of altering their responsiveness to VM-associated, diffusible Slit proteins, even in the absence of FP contact.

The role of FP contact in commissural axon pathfinding

In previous studies of mouse, *Xenopus*, and zebrafish embryos that lack a FP or both a notochord and a FP, most commissural axons were reported to follow wild-type-like trajectories to the VM. Within the VM, however, these axons displayed a variety of guidance errors (Bernhardt et al., 1992; Bovolenta and Dodd, 1991; Greenspoon et al., 1995; Hatta, 1992; Matise et al., 1999). In FP-lacking, *gli2*-deficient mouse

embryos, for example, many commissural axons either stalled at the VM or inappropriately projected in the caudal direction (Matise et al., 1999). The latter observation presumably reflects the loss of FP-associated Wingless-type (Wnt) and Shh, which have recently been shown to facilitate the rostral turn executed by decussated commissural axons in wild-type vertebrate embryos (Bourikas et al., 2005; Lyuksyutova et al., 2003).

In manipulated *Xenopus* embryos that lack both a FP and a notochord, commissural axons erroneously projected through the VM at less than a 90 degree angle (Clarke et al., 1991). We observed a similar phenotype in *gli2*$^{-/-}$ embryos and cultured FP-lacking explants (see Figs. 1 and 4). It is important to note in this regard that the cultured FP-excised explants we employed lack both a FP and a notochord, whereas the *gli2* homozygotes retain a notochord. Therefore, collectively, our results imply that, at least for some commissural axons, FP contact, but not diffusible notochord-derived guidance cues, is required for the prototypic orthogonal turn they execute after reaching the VM. This is consistent with the behavior of commissural axons in cultured rodent hindbrain explants (Shirasaki and Murakami, 2001).

Prior to this study, a role for FP contact in regulating the post-crossing behavior of commissural axons had only been assessed in lower vertebrates. Interestingly, an analysis of FP-lacking zebrafish mutants revealed that 43% of CoPA axons elaborated wild-type projections on the contralateral side of the VM (Bernhardt et al., 1992; Greenspoon et al., 1995; Hatta, 1992). Since these axons grew along a diagonal trajectory into intermediate regions of the mutant spinal cord, both their expulsion out of the VM and their ability to adopt a unique post-crossing trajectory was clearly not dependent on FP contact. Consistent with these observations, we show here that despite the presence of some aberrant contralateral projections, a significant number of ILC axons (counterparts of zebrafish CoPA axons) follow wild-type-like contralateral trajectories in *gli2*-deficient mouse embryos (14/44 cohorts; see Table) and in cultured FP-lacking spinal cord explants (19/21 explants). Thus, in both fish and mammals, while the post-crossing behavior of some commissural axons is clearly dependent on FP contact, other axons are able to leave the VM and elaborate appropriate contralateral projections even without experiencing contact with FP cells.

We recently described four distinct contralateral commissural projections in the wild-type embryonic mouse spinal cord (see Fig. 1, Schematic A). To determine whether FP contact is required for the elaboration of these projections, we used a focal DiI analysis to score the numbers of MLC, ILC, BLC, and FTC axons contained within cohorts of commissural axons in heterozygous and homozygous *gli2* mutant embryos. These analyses revealed the presence of each of the four projection patterns, suggesting that even in the absence of FP contact, some commissural axons can adopt a variety of post-crossing trajectories. It is important to note in this regard, however, that the frequencies at which each projection pattern is observed in *gli2* null embryos differ from those observed in heterozygous littermates (Table 1). For instance, in spinal cords derived from *gli2* homozygous mutants, the percentage of contralateral trajectories containing MLC axons is approximately double (41%; 15/37 trajectories) the frequency observed in heterozygous littermates (20%; 16/81 trajectories). Interestingly, we also observed a slight increase in the frequency of MLC projections in cultured, FP-lacking explants dissected from wild-type embryos (30%; 18/58 trajectories), compared to intact (FP-containing) open book preparations derived from wild-type embryos of a comparable developmental stage, in vivo (Kadison and Kaprielian, 2004). On the contrary, the percentage of trajectories displaying BLC axons in *gli2* null embryos (15%; 12/81 trajectories) and *gli2* heterozygotes (11%; 4/37 trajectories) is quite comparable, and this was also the case for the cultured, FP-lacking explants. These data suggest that distinct contralateral projections may have differential requirements for FP contact and FP-derived cues. Therefore, not only the shape but also the frequency of contralateral projection patterns may be dependent on FP contact, and the degree of this dependency may vary among trajectories. In a complementary approach to the focal DiI analyses, we used confocal microscopy on crystal DiI-labeled preparations in order to ask whether the topography of the various contralateral commissural projections is preserved in the spinal cords of *gli2* null embryos. This analysis largely confirmed that MLC, ILC, BLC and FTC axons were segregated to the same planes of the Z-axis in *gli2* homozygous embryos as they are in heterozygous and wild-type littermates. However, the topography of MLC and ILC projections was better preserved than the organization of the BLC and FTC projections. Notably, we also observed a paucity of FTC axons in *gli2*$^{-/-}$ embryos, as compared to age-matched heterozygous littermates (due to technical reasons, this was not the case for cultured, FP-lacking explants; see Results). A plausible explanation for this finding is that FTC axons may selectively require FP-derived trophic support (Wang and Tessier-Lavigne, 1999) or that they may be more reliant on FP-derived signals than the other contralateral commissural trajectories (as discussed above).

The role of contact-dependent guidance cues and glia at the ventral midline

In wild-type vertebrate embryos, the local guidance of commissural axons at the VM is mediated through the expression of contact-dependent cues, such as NrCAM, nectins, and ephrins, which are located on the surface of FP cells (Imondi et al., 2000; Okabe et al., 2004; Stoeckli et al., 1997). Not unexpectedly, it was previously shown that NrCAM is absent from the spinal cord midline of *gli2* null embryos. Interestingly, NrCAM is expressed at a constant level on pre- and post-crossing commissural axons in the homozygous embryo, whereas the level of expression on commissural axons in heterozygous littermates is markedly upregulated as these axons cross through the NrCAM-rich FP (Matise et al., 1999). These results suggest a potential mechanism through which FP cells may directly play a role in contact-mediated guidance. Specifically, some factors on both FP cells and axons (e.g., NrCAM) may rely on heterologous cell–cell interactions at the VM for a proper balance of expression, which may

involve the transfer of molecules from the surface of FP cells to decussating commissural axons, and a small number of studies provide evidence for this model (Campbell and Peterson, 1993; Okabe et al., 2004). Here, we show that, in the absence of FP contact and FP-derived contact-dependent guidance cues, a large number of commissural axons appear to appropriately decussate, upregulate post-crossing receptors, and form longitudinal tracts. These results imply that local control by FP-derived cues does not appear to be absolutely required for the proper cell surface protein expression and the contralateral pathfinding of commissural axons in the embryonic mouse spinal cord. On the other hand, the failure of a subset of commissural axons in *gli2* homozygotes to form an organized ventral commissure and execute prototypic orthogonal turns at the VM suggests that there is clearly some loss of local, contact-mediated guidance at the ventral midline (see Supplemental Fig. 2), and that the relevant cues are perhaps important for proper fasciculation/tract formation at the VM (see below; Supplemental Fig. 3; Matise et al., 1999).

Midline-associated glial cells also appear to be a source of contact-dependent or diffusible guidance cues for commissural axons in a variety of systems. For example, at the optic chiasm (Marcus et al., 1995), and in the immediate vicinity of the anterior commissure (Cummings et al., 1997) and corpus callosum (Shu and Richards, 2001), glial cells have been shown to act as intermediate targets for midline-crossing axons. Therefore, it seems possible that, in the *gli2* mutant mouse spinal cord, radial glia located within the ventral ventricular zone (McDermott et al., 2005) express Slit and Netrin-1 and that the close proximity of these cells to, or their contact with, growing commissural axons facilitates proper pathfinding in the absence of a FP. Consistent with this hypothesis, glial cells have recently been implicated in the fasciculation of commissural axons within the ventral commissure (Lane et al., 2004).

The role of FP contact in altering the responsiveness of commissural axons

Decussated commissural axons must perceive the once attractive VM as an inhibitory environment if they are to extend along the next leg of their journey. Accordingly, commissural axons lose responsiveness to Netrin-1 (Shirasaki et al., 1998) and gain responsiveness to the midline repellents, Slit2 and Sema3B/3F only after they contact FP cells in vitro (Zou et al., 2000). Presumably, these changes help drive decussated commissural axons out of the VM and into longitudinal tracts in vivo. We show here that, even in *gli2* homozygous mouse embryos, some commissural axons are able to escape the VM and turn into the longitudinal plane. This raised the possibility that repellent guidance cues are localized to the VM in *gli2* null embryos, and that commissural axons, which have never experienced FP contact, are capable of altering their responsiveness to these cues. Consistent with this hypothesis, *slit1-3* is expressed within the ventral ventricular zone (potentially midline glial cells—see above) and by motoneurons, and their receptors, Robo1 and Robo2, are selectively expressed on longitudinal axon tracts in *gli2* homozygotes. While VM-associated Slits presumably expel Robo-positive axons out of the midline area (see Fig. 7) motoneuron-derived Slits may subsequently hem decussated commissural axons into longitudinal axon tracts in both wild-type and mutant animals.

As a first step towards directly determining whether FP contact is required to alter the responsiveness of commissural axons in mouse embryos, we asked whether axons emerging from FP-attached half, open book explants were selectively responsive to sources of Slit proteins. This collagen gel co-culture system has previously been used to demonstrate that rat commissural axons gain responsiveness to Slits only after they encounter FP cells (Zou et al., 2000). In contrast, however, we found that commissural axons emerging from a FP-lacking half spinal cord explant derived from a mouse embryo were repelled by Slits (data not shown). While these apparently inconsistent results could simply reflect species-specific responsivity profiles, it is interesting to note that pre-crossing commissural axons emanating from chick dorsal spinal cord explants are also repelled by Slit proteins in vitro (Mambetisaeva et al., 2005). Although we were not able to use this particular assay to directly demonstrate that commissural axons alter their responsiveness to VM-associated repellent guidance cues in the absence of FP contact, we have shown that a significant number of commissural axons fail to leave the VM in cultured, Robo/Fc-treated FP-lacking explants. These results, together with our in vivo expression data, suggest that many spinal commissural axons are capable of upregulating Robo receptors and becoming responsive to VM-derived Slits in FP-lacking spinal cords. It is interesting to note in this regard that naïve commissural growth cones, which have never contacted a FP, also gain responsiveness to exogenously applied, diffusible Slit in the *Xenopus* turning assay, in vitro. Taken all together, these findings underscore an important functional role for Robo-Slit interactions that is separable from the role of FP contact in altering the responsiveness of contralateral commissural projections.

Despite our finding that some commissural axons appear to become responsive to Slit and elaborate wild-type-like contralateral projections without encountering a FP, other axons fail to leave the VM and commit a variety of pathfinding errors in the absence of FP contact. Presumably, this latter group of axons is unable to alter their responsiveness to VM-associated guidance cues, potentially because they do not express Robo receptors on their growth cones and, therefore, cannot effectively "silence" Netrin attraction at the VM. An alternative possibility is that Rig-1 expression, which is not properly extinguished on commissural axons as they reach the VM in *gli2* homozygotes, maintains the presumed unresponsivity of these axons to midline-derived Slits.

Experience-independent midline guidance?

Our findings support the existence of at least two broad subclasses of spinal commissural axons, which either require or do not require FP contact in order to adopt appropriate contralateral trajectories. That some commissural axons are capable of elaborating appropriately shaped contralateral projections in the absence of prior FP contact, both in vitro and in vivo, raises the

possibility that experience-independent mechanisms may play a role in regulating the pathfinding of some midline-crossing axons in the developing CNS. Consistent with this model, motor axons, which fail to cross the midline in *Drosophila comm* mutants, elaborate mirror-image wild-type-like projections and ultimately reach their appropriate muscle targets (Wolf and Chiba, 2000). Similarly, in *rig-1* homozygous mouse embryos, pontine and lateral reticular/external cuneate nuclei neurons project axons to their correct cerebellar targets, even though they fail to decussate/contact FP cells (Marillat et al., 2004).

An intrinsic clock that regulates the timing of pathfinding decisions, presumably through the temporally and spatially precise deployment of specific guidance receptors, could underlie an experience-independent model of axon guidance. Our finding that Robo receptors are selectively expressed on decussated segments of commissural axons in *gli2*$^{-/-}$ embryos is consistent with this model, as are several in vitro and in vivo observations made in a variety of guidance systems. For example, the responsiveness of cultured *Xenopus* retinal ganglion cell (RGC) axons to Netrin-1 was shown to be dependent on the developmental stage at which the neurons were isolated/tested, rather than their previous experiences (Shewan et al., 2002). In the *Drosophila* CNS, *comm* expression in commissural neurons is under strict spatial and temporal control and is closely linked with midline crossing. Specifically, *comm* is "on" in commissural neurons only during the time when their corresponding axons are in the act of decussating. Importantly, once these axons have reached the contralateral side of the midline, *comm* expression is extinguished. Ipsilateral axons on the other hand, whose axons do not cross the midline, never express *comm* (Georgiou and Tear, 2002; Keleman et al., 2002, 2005). Thus, Comm appears to act cell autonomously to regulate midline crossing of commissural axons. Taken together with our findings, these observations suggest that intrinsic mechanisms may control several aspects of axon guidance.

Acknowledgments

We gratefully thank Kosta Dobrenis and Joe Zavilowitz for their assistance with confocal microscopy, A. Whitham for generating the schematic illustrations, Cuiling Wang, Mimi Kim, and Alexander Harris for their assistance with statistical analyses, and C. Mason (Columbia), C. Lang (Columbia), L. Erskine (University College London), A. Dillon, S. Reeber, N. Sakai, C. Aguirre-Chen, E. Carlin, and A. Bravo for critically reading the manuscript. We are especially grateful to C.-M. Fan (Carnegie Institute) for providing *gli2* breeding pairs and Dritan Agalliu for genotyping the *nkx2.2* mouse embryos. The monoclonal antibodies 2H3 and 4D7 were obtained from the Developmental Studies Hybridoma Bank developed under the auspices of the NICHD and maintained by The University of Iowa, Department of Biological Sciences, Iowa City, IA 52242. This work was aided by grants from the NIH (R01 NS 38505) and the New Jersey Commission on Spinal Cord Research (05-3042-SCR-E-0) to Z.K.

Appendix A. Supplementary data

Supplementary data associated with this article can be found, in the online version, at doi:10.1016/j.ydbio.2006.06.022.

References

Bernhardt, R., Nguyen, N., Kuwada, J., 1992. Growth cone guidance by floor plate cells in the spinal cord of zebrafish embryos. Neuron 8, 869–882.

Bourikas, D., Pekarik, V., Baeriswyl, T., Grunkditz, A., Sadhu, R., Nardo, M., Stoeckli, E., 2005. Sonic hedgehog guides commissural axons along the longitudinal axis of the spinal cord. Nat. Neurosci. 8, 297–304.

Bovolenta, P., Dodd, J., 1991. Perturbation of neuronal differentiation and axon guidance in the spinal cord of mouse embryos lacking a floor plate: analysis of Danforth's short tail mutation. Development 113, 625–639.

Briscoe, J., Sussel, L., Serup, P., Hartigan-O'Connor, D., Jessell, T.M., Rubinstein, J.L., Ericson, J., 1999. Homeobox gene Nkx2.2 and specification of neuronal identity by graded Sonic hedgehog signalling. Nature 398, 622–627.

Brittis, P.A., Lu, Q., Flanagan, J.G., 2002. Axonal protein synthesis provides a mechanism for localized regulation at an intermediate target. Cell 110, 223–235.

Brose, K., Bland, K.S., Wang, K.H., Arnott, D., Henzel, W., Goodman, C.S., Tessier-Lavigne, M., Kidd, T., 1999. Slit proteins bind Robo receptors and have an evolutionarily conserved role in repulsive axon guidance. Cell 96, 795–806.

Campbell, R.M., Peterson, A.C., 1993. Expression of a lacZ transgene reveals floor plate cell morphology and macromolecular transfer to commissural axons. Development 119, 1217–1228.

Charron, F., Stein, E., Jeong, J., McMahon, A., Tessier-Lavigne, M., 2003. The morphogen Sonic Hedgehog is an axonal chemoattractant that collaborates with Netrin-1 in midline axon guidance. Cell 113, 11–23.

Clarke, J.D.W., Holder, N., Soffe, S.R., Storm-Mathisen, J., 1991. Neuroanatomical and functional analysis of neural tube formation in notochordless *Xenopus* embryos: laterality of the ventral spinal cord is lost. Development 112, 499–516.

Cummings, D., Malun, D., Brujnes, P., 1997. Development of the anterior commissure in the opossum: midline extracellular space and glia coincide with early axon decussation. J. Neurobiol. 32, 403–414.

Dillon, A., Fujita, S., Matise, M., Jarjour, A., Kennedy, T., Kollmus, H., Arnold, H., Weiner, J., Sanes, L., Kaprielian, Z., 2005. Molecular control of spinal accessory motor neuron/axon development in the mouse spinal cord. J. Neurosci. 25, 10119–10130.

Ding, Q., Motoyama, J., Gasca, S., Mo, R., Sasaki, H., Rossant, J., Hui, C., 1998. Diminished Sonic hedgehog signaling and lack of floor plate differentiation in Gli2 mutant mice. Development 125, 243–253.

Dodd, J., Morton, S.B., Karagogeos, D., Yamamoto, M., Jessell, T.M., 1988. Spatial regulation of axonal glycoprotein expression on subsets of embryonic spinal neurons. Neuron 1, 105–116.

Fazeli, A., Dickinson, S.L., Hermiston, M.L., Tighe, R.V., Steen, R.G., Small, C.G., Stoeckli, E.T., Keino-Masu, K., Masu, M., Rayburn, H., Simons, J., Bronson, R.T., Gordon, J.I., Tessier-Lavigne, M., Weinberg, R.A., 1997. Phenotype of mice lacking functional Deleted in Colorectal Carcinoma (DCC) gene. Nature 386, 796–804.

Georgiou, M., Tear, G., 2002. Commissureless is required both in commissural neurons and midline cells for axon guidance across the midline. Development 129, 2947–2956.

Greenspoon, S., Patel, C., Hashmi, S., Bernhardt, R., Kuwada, J., 1995. The notochord and floor plate guide growth cones in the zebrafish spinal cord. J. Neurosci. 15, 5956–5965.

Hatta, K., 1992. Role of the floor plate in axonal patterning in the zebrafish CNS. Neuron 9, 629–642.

Imondi, R., Kaprielian, Z., 2001. Commissural axon pathfinding on the contralateral side of the floor plate: a role for B-class ephrins in specifying the dorsoventral position of longitudinally-projecting commissural axons. Development 128, 4859–4871.

Imondi, R., Wideman, C., Kaprielian, Z., 2000. Complementary expression of transmembrane ephrins and their receptors in the mouse spinal cord: a possible role in constraining the orientation of longitudinally projecting axons. Development 127, 1397–1410.

Jen, J., Chan, W., Bosley, T., Wan, J., Carr, J., Rub, U., Shattuck, D., Salamon, G., Kudo, L., Ou, J., Lin, D., Salih, M., Kansu, T., Dhalaa, H.A., et al., 2004. Mutations in the human Robo gene disrupt hindbrain axon pathway crossing and morphogenesis. Science 304, 1509–1513.

Jevince, A., Kadison, S., Pittman, A., Chien, C.-B., Kaprielian, Z., 2006. Distribution of EphB receptors and ephrin-B1 in the developing vertebrate spinal cord. J. Comp. Neurol. 497, 734–750.

Kadison, S.R., Kaprielian, Z., 2004. Diversity of contralateral commissural projections in the embryonic rodent spinal cord. J. Comp. Neurol. 472, 411–422.

Kaprielian, Z., Cho, K.-O., Hadjiargyrou, M., Patterson, P.H., 1995. CD9, a major platelet cell surface glycoprotein, is a ROCA antigen and is expressed in the nervous system. J. Neurosci. 15, 562–573.

Kaprielian, Z., Runko, E., Imondi, R., 2001. Axon guidance at the midline choice point. Dev. Dyn. 221, 154–181.

Keleman, K., Rajagopalan, S., Cleppien, D., Ties, D., Paiha, K., Huber, L.A., Technau, G.M., Dickson, B.J., 2002. Comm sorts Robo to control axon guidance at the *Drosophila* midline. Cell 110, 415–427.

Keleman, K., Ribeiro, C., Dickson, B., 2005. Comm functions in commissural axon guidance: cell-autonomous sorting of Robo *in vivo*. Nat. Neurosci. 8, 156–163.

Kidd, T., Brose, K., Mitchell, K.J., Fetter, R.D., Tessier-Lavigne, M., Goodman, C.S., Tear, G., 1998. Roundabout controls axon crossing of the CNS midline and defines a novel subfamily of evolutionarily conserved guidance receptors. Cell 92, 205–215.

Kidd, T., Bland, K.S., Goodman, C.S., 1999. Slit is the midline repellent for the Robo receptor in *Drosophila*. Cell 96, 785–794.

Lane, S., McDermott, K., Dockery, P., Fraher, J., 2004. The developing cervical spinal ventral commissure of the rat: a highly controlled axon-glial system. J. Neurocytol. 33, 489–501.

Li, H.-s., Chen, J.-h., Wu, W., Fagaly, T., Zhou, L., Yuan, W., Dupuis, S., Jiang, Z.-h., Nash, W., Gick, C., Ornitz, D.M., Wu, J.Y., Rao, Y., 1999. Vertebrate Slit, a secreted ligand for the transmembrane protein roundabout is a repellent for olfactory bulb axons. Cell 96, 807–818.

Long, H., Sabatier, C., Ma, L., Plump, A., Yuan, W., Ornitz, D.M., Tamada, A., Murakami, F., Goodman, C.S., Tessier-Lavigne, M., 2004. Conserved roles for Slit and Robo proteins in midline commissural axon guidance. Neuron 42, 213–223.

Lyuksyutova, A.I., Lu, C.-C., Milanesio, N., King, L.A., Guo, N., Wang, Y., Nathans, J., Tessier-Lavigne, M., Zou, Y., 2003. Anterior–posterior guidance of commissural axons by Wnt-Frizzled signaling. Science 302, 1984–1988.

Mambetisaeva, E., Andrews, W., Camurri, L., Annan, A., Sundaresan, V., 2005. Robo family of proteins exhibit differential expression in mouse spinal cord and Robo-Slit interaction is required for midline crossing in vertebrate spinal cord. Dev. Dyn. 233, 41–51.

Marcus, R., Blazeski, R., Godement, P., Mason, C., 1995. Retinal axon divergence in the optic chiasm: uncrossed axons diverge from crossed axons within a midline glial specialization. J. Neurosci. 15, 3716–3729.

Marillat, V., Sabatier, C., Failli, V., Matsunaga, E., Sotelo, C., Tessier-Lavigne, M., Chedotal, A., 2004. The Slit receptor Rig-1/Robo3 controls midline crossing by hindbrain precerebellar neurons and axons. Neuron 43, 69–79.

Matise, M.P., Epstein, D.J., Park, H.L., Platt, K.A., Joyner, A.L., 1998. Gli 2 is required for induction of floor plate and adjacent cells, but not most ventral neurons in the mouse central nervous system. Development 125, 2759–2770.

Matise, M.P., Lustig, M., Sakurai, T., Grumet, M., Joyner, A.L., 1999. Ventral midline cells are required for the local control of commissural axon guidance in the mouse spinal cord. Development 126, 3649–3659.

McDermott, K., Barry, D., McMahon, S., 2005. Role of radial glia in cytogenesis, patterning and boundary formation in the developing spinal cord. J. Anat. 207, 241–250.

Mo, R., Freer, A., Zinyk, D., Crackower, M., Michaud, J., Heng, H.-Q., Chik, K., Shi, X.-M., Tsui, L.-C., Cheng, S., Joyner, A., Hui, C.-c., 1997. Specific and redundant functions of Gli2 and Gli3 zinc finger genes in skeletal patterning and development. Development 124, 113–123.

Moos, M., Tacke, R., Scherer, H., Teplow, D., Fruh, K., Schachner, M., 1988. Neural adhesion molecule L1 as a member of the immunoglobulin superfamily with binding domains similar to fibronectin. Nature 334, 701–703.

Nissen, U., Mochida, H., Glover, J., 2005. Development of projection-specific interneurons and projection neurons in the embryonic mouse and rat spinal cord. J. Comp. Neurol. 483, 30–47.

Okabe, N., Shimizu, K., Ozaki-Kuroda, K., Nakanishi, H., Morimoto, K., Takeuchi, M., Katsumaru, H., Murakami, F., Takai, Y., 2004. Contacts between the commissural axons and the floor plate cells are mediated by nectins. Dev. Biol. 273, 244–256.

Patel, K., Nash, J.A., Itoh, A., Liu, Z., Sundaresan, V., Pini, A., 2001. Slit proteins are not dominant chemorepellents for olfactory tract and spinal motor axons. Development 128, 5031–5037.

Rajagopalan, S., Vivancos, V., Nicolas, E., Dickson, B.J., 2000. Selecting a longitudinal pathway: robo receptors specify the lateral position of axons in the *Drosophila* CNS. Cell 103, 1033–1045.

Sabatier, C., Plump, A., Ma, L., Brose, K., Tamada, A., Murakami, F., Lee, E., Tessier-Lavigne, M., 2004. The divergent Robo family protein Rig-1/Robo3 is a negative regulator of Slit responsiveness required for midline crossing by commissural axons. Cell 117, 157–169.

Schubert, W., Kaprielian, Z., 2001. Identification and characterization of a cell surface marker for embryonic rat spinal accessory motor neurons. J. Comp. Neurol. 439, 368–383.

Shewan, D., Dwivedy, A., Anderson, R., Holt, C., 2002. Age-related changes underlie switch in netrin-1 responsiveness as growth cones advance along visual pathway. Nat. Neurosci. 5, 955–962.

Shirasaki, R., Murakami, F., 2001. Crossing the floor plate triggers sharp turning of commissural axons. Dev. Biol. 236, 99–108.

Shirasaki, R., Katsumata, R., Murakami, F., 1998. Change in chemoattractant responsiveness of developing axons at an intermediate target. Science 279, 105–107.

Shu, T., Richards, L., 2001. Cortical axon guidance by the glial wedge during the development of the corpus callosum. J. Neurosci. 21, 2749–2758.

Simpson, J.H., Bland, K.S., Fetter, R.D., Goodman, C.S., 2000. Short-range and long-range guidance by slit and its robo receptors: a combinatorial code of robo receptors controls lateral position. Cell 103, 1019–1032.

Stein, E., Tessier-Lavigne, M., 2001. Hierarchial organization of guidance receptors: silencing of netrin attraction by Slit through a Robo/DCC receptor complex. Science 291, 1928–1938.

Stoeckli, E., Sondregger, P., Pollerberg, G., Landmesser, L., 1997. Interference with Axonin1 and NrCAM interactions unmasks a floor plate-activity inhibitory for commissural axons. Neuron 18, 209–221.

Wang, H., Tessier-Lavigne, M., 1999. En passant neurotrophic action of an intermediate axonal target in the developing mammalian CNS. Nature 401, 765–769.

Wolf, B.D., Chiba, A., 2000. Axon pathfinding proceeds normally despite disrupted growth cone decisions at CNS midline. Development 127, 2001–2009.

Zou, Y., Stoeckli, E., Chen, H., Tessier-Lavigne, M., 2000. Squeezing axons out of the gray matter: a role for slit and semaphorin proteins from midline and ventral spinal cord. Cell 102, 363–375.